Arabian Journal of Chemistry (2020) 13, 5788–5799

King Saud University

Arabian Journal of Chemistry

www.ksu.edu.sa
www.sciencedirect.com

ORIGINAL ARTICLE

Evaluation of the catalytic effect of ZnO as a secondary phase in the $Ni_{0.5}Zn_{0.5}Fe_2O_4$ system and of the stirring mechanism on biodiesel production reaction

Ana F.F. Farias [a,*], Deisy T. de Araújo [a], Adriano L. da Silva [a], Elvia Leal [a], José G.A. Pacheco [b], Manoel R. Silva [c], Ruth H.G.A. Kiminami [d], Ana C.F. de M. Costa [a]

[a] *Federal University of Campina Grande/UFCG, Synthesis of Ceramic Materials Laboratory – LabSMaC, Science and Engineering of Materials Postgraduate, Aprígio Veloso Avenue –882, Bodocongó, 58109-970 Campina Grande, PB, Brazil*
[b] *Federal University of Pernambuco (UFPE), Department of Chemical Engineering, Laboratory of Refining and Cleaner Technology (LATECLIM), Institute for Petroleum and Energy Research (LITPEG), 50740-550 Recife, PE, Brazil*
[c] *Federal University of Itajubá/UNIFEI, Department of Physics and Chemistry, Institute of Sciences, Av. B. P. S., 1303, Pinheirinho, 37500-903 Itajubá, MG, Brazil*
[d] *Federal University of São Carlos/UFSCar, Department of Materials Engineering, 13565-905 São Carlos, SP, Brazil*

Received 13 December 2019; accepted 15 April 2020
Available online 23 April 2020

KEYWORDS

Magnetic catalysts;
Ni-Zn ferrite;
Zinc oxide;
Transesterification;
Biodiesel

Abstract In search of efficient ways to produce biodiesel under environmentally friendly conditions, catalytic reactions have been explored with emphasis on replacing homogeneous by heterogeneous catalysis with the use of new catalyst types, such as the spinel ferrites, which are described as a viable option, since they are stable, highly active, inexpensive, reusable, and allow the easy recovery of the reaction medium through the application of magnetic fields. In this context, the present work proposes to contribute to the consolidation of the catalytic viability of the $Ni_{0.5}Zn_{0.5}Fe_2O_4$ system obtained by combustion reaction, because although previous studies indicate the catalytic effectiveness of this system in polyphasic form, the present work seeks as differential to evaluate the influence of the secondary phases and magnetization of the Ni-Zn system in the conversion to biodiesel, and for this purpose, it aims to evaluate the catalytic effect of ZnO formed as secondary phase and obtained concomitantly in the Ni-Zn ferrite synthesis, besides

* Corresponding author.
E-mail address: anafffr@hotmail.com (A.F.F. Farias).
Peer review under responsibility of King Saud University.

Production and hosting by Elsevier

https://doi.org/10.1016/j.arabjc.2020.04.016

evaluating the effect of the stirring mechanism used in biodiesel production reaction by the ethyl transesterification of soybean oil. The synthesized Ni-Zn ferrites and ZnO sample were characterized by X-ray diffraction (XRD), nitrogen adsorption textural analysis (BET), particle size distribution, and then, tested in two reactor types, one with magnetic stirring, and another of mechanical stirring, to observe the magnetization effect of the material, and the characterization of the obtained biodiesels by gas chromatography (GC) and acidity index. The performed catalytic tests showed that the Ni-Zn ferrites promoted excellent ester conversions with values near and above 94%, thus confirming that although ZnO also promotes good ester conversion (83.9%), the catalytic effectiveness of the Ni-Zn ferrite is evident and independent of secondary phases. Moreover, the catalytic tests performed in the magnetic stirring reactor using the Ni-Zn ferrites as catalysts made it possible to realize that their magnetic properties may be interference in the catalytic effectiveness, being this, a more determining factor than the surface characteristics.

1. Introduction

Biodiesel is a biofuel obtained from edible or inedible vegetable oils, waste oils and animal fats, and recognized for its advantages such as being renewable, biodegradable, low environmental toxicity and higher combustion efficiency (Avhad & Marchetti, 2015). It is already a worldwide reality and is conventionally produced *via* transesterification or esterification of vegetable oils or animal fats with methanol in the presence of acidic and basic homogeneous catalysts (Ali et al., 2018; Shan et al., 2018). Due to the scarcity of fossil resources and environmental concerns such as greenhouse gas emissions, biodiesel has been steadily gaining attention as it is considered a promising substitute for petroleum diesel in the near future (Shan et al., 2018).

Although homogeneous catalysis conventionally used in biodiesel production (catalysts: basic – NaOH/KOH; acidic - H_2SO_4) offers high yields under moderate conditions, they are associated with several limitations and disadvantages such as extra neutralization step, high production cost due to the purification process, and wastewater generation that needs treatment (Ali et al., 2018; Guldhe et al., 2017; Ullah et al., 2018). Due to the mentioned problems and the need for the development and optimization of environmentally friendly chemical biodiesel production processes, studies have been conducted in favor of the development of innovative processes involving the replacement of homogeneous catalysis by the use of heterogeneous catalytic reactions based on new inorganic solid catalysts.

In this context, recent researches have reported the use of ternary oxides such as spinel-type ferrites as a promising proposal for application in the heterogeneous catalysis for biodiesel production (Pereira et al., 2015; Dantas et al., 2016; Dantas et al., 2017; Falcão et al., 2018; Alaei et al., 2018; Ashok & Kennedy, 2019; Ashok et al., 2019; Mapossa et al., 2020), since they have structural and magnetic properties that turn enable the separation by magnetization, reducing the material loss, and making possible the recovery and reuse of these solid catalysts; in addition, they accelerate the purification step of the final reaction product, as they do not cause emulsion formation in the reaction mixture, and consequently generate less effluents (Carrera et al., 2013; Lee et al., 2014; Pereira et al., 2015; Shan et al., 2018; Ali et al., 2018; Tang et al., 2018).

Recent researches (Dantas et al., 2016; Dantas et al., 2017; Dantas et al., 2018) indicate that Ni-Zn ferrite presents ideal criteria for catalysis because it has nanostructural characteristics and, therefore, a high surface area, with values between 48.89 and 65.28 $m^2\ g^{-1}$ (Dantas et al., 2017; Dantas et al., 2018), and thus, greater amounts of active chemical sites to participate in the reactions. A highlight for the study of (Dantas et al. 2018), that using as catalyst the Ni-Zn nanoferrite obtained in the large-scale polyphasic form ($Ni_{0.5}Zn_{0.5}Fe_2O_4/Fe_2O_3/ZnO$) by combustion reaction, proved the high catalytic activity of this system in the production of biodiesel with conversion of 99.4% in methyl and ethyl esters.

Autocombustion synthesis is a consolidated method that has also been receiving substantial attention in studies (Prasad et al., 2014; Chagas et al., 2014; Lazarova et al., 2019) because it is practical, fast, with satisfactory yields, and for allowing the obtaining of single-phase material. There are researches that attribute the synthesis of the $Ni_{0.5}Zn_{0.5}Fe_2O_4$ system *via* combustion reaction and still use post-reaction heat treatments and/or simple changes in the amount of fuel, amount of heat supplied at the time of the reaction (Phadatare et al., 2013; Chagas et al., 2014; Chauhan et al., 2016; Lazarova et al., 2019), due to the need to eliminate low crystallinity secondary phases as ZnO and/or hematite, seeking to obtain the phase of interest, Ni-Zn ferrite as a single phase material, and thus reducing the interference factors in their applications.

There are also studies of the application of zinc oxide in its pure form, doped or as a support in the biodiesel production (Liu & Zhang, 2011; Farias et al., 2015; Buchori et al., 2017; Baskar et al., 2018), presenting promising results in catalysis, and leading to conversions of up to 96%, depending on the synthesis method for its obtaining, and of the reaction conditions during transesterification (Liu & Zhang, 2011; Farias et al., 2015). Many synthesis techniques of nanometric or micrometric ZnO have been investigated in the literature, such as vapor deposition, electrochemical deposition, co-precipitation, sol–gel, solvothermal, hydrothermal, microwave assisted hydrothermal technique, thermal decomposition, combustion synthesis and sonochemistry synthesis (Lamba et al., 2019). However, there is limited literature on pure ZnO obtained by combustion for application in biodiesel synthesis by transesterification reaction (Lamba et al., 2019).

Thus, it is relevant to investigate the feasibility of using the zinc oxide obtained by combustion reaction in heterogeneous catalysis and also to understand the critical factor effect, such as the existence of ZnO as secondary phases in the composition of Ni-Zn ferrites, as this may be determinant in the characteristics and properties of ferrite and may consequently be a significant influence on the catalytic effect when applied to biodiesel production.

In this context, the present article seeks to contribute to the consolidation of the large-scale obtainment of the single-phase $Ni_{0.5}Zn_{0.5}Fe_2O_4$ system and of the pure ZnO by combustion reaction, as well as to prove the catalytic viability of each one, and thus answer some questions about the effect of the presence of the secondary phase of zinc oxide formed concomitantly in the synthesis of Ni-Zn ferrite on the catalytic activity. In addition, the present study intends to evaluate in more detail the effect of the reaction stirring mechanism used in biodiesel production (mechanical and magnetic), and thus the possible interference of the magnetic property in the conversion of soybean oil to ethyl esters through the transesterification reaction.

2. Materials and methods

2.1. Materials

For the production of the catalysts $Ni_{0.5}Zn_{0.5}Fe_2O_4$ and ZnO, it was used a stainless-steel container with a batch production capacity of 200 g/product and the following reagents: nickel (II) nitrate hexahydrate, (Dynamics - Brazil) - $Ni(NO_3)_2{\cdot}6H_2O$ (99%), zinc(II) nitrate hexahydrate (Dynamics – Brazil) - $Zn(NO_3)_2{\cdot}6H_2O$ (98%), iron(III) nitrate nonahydrate, (Dynamics – Brazil) - $Fe(NO_3)_3{\cdot}9H_2O$ (99%), and urea, (Neon – Brazil) - $CO(NH_2)_2$ (98%).

The catalytic performance of the $Ni_{0.5}Zn_{0.5}Fe_2O_4$ systems obtained in polyphase/diphasic/single phase forms, and also of ZnO were evaluated in biodiesel production by transesterification reaction of commercial (SOYA – Brazil) soybean oil in the presence of ethanol, Dynamics - Brazil (99,8%).

2.2. Methods

2.2.1. Synthesis of the catalysts

The reactional stoichiometric composition of $Ni_{0.5}Zn_{0.5}Fe_2O_4$ and ZnO ceramic materials for synthesis by combustion reaction by was based on the total valence of oxidizing and reducing reagents using concepts from propellant and explosive chemistry (Jain et al., 1981). The syntheses were performed using two heating systems (reactors), first the standard device designed for the production of ceramic nanomaterials on a large scale by combustion reaction, belonging to the pilot plant referring to the patent BR 10 2012 002181–3 (Costa & Kiminami, 2012), and a second heating reactor (which was used also to obtain the ZnO phase), seeking to increase the heating power to reach combustion temperatures higher than those observed in the study of Dantas et al. (2020), which was served as a reproducibility parameter of the $Ni_{0.5}Zn_{0.5}Fe_2O_4$ system synthesis reactions. The reactions were performed seeking to produce ceramic nanomaterials single-phases of Ni-Zn ferrite and ZnO directly from the combustion reaction.

2.2.2. Catalytic evaluation of the catalysts

The synthesis of biodiesel was performed in triplicate using reaction conditions optimized by (Dantas et al., 2018): 180 °C temperature and 1 h reaction time, oil: alcohol molar ratio of 1:15, and 3% of catalyst to oil mass (30 g).

Initially, the ferrite tests as catalysts were conducted in a stainless-steel reactor, which holds an 80-mL borosilicate beaker under pressure, using magnetic stirring, and heating promoted by an electric resistance plate. The catalysts after catalytic testing were separated by centrifugation, and the catalytic test product (biodiesel) was washed with distilled water at approximately 60 °C, oven dried and characterized.

In order to study the catalytic behavior of the catalysts, eliminating the possible magnetic interference, it was also proposed to perform the catalytic tests of Ni-Zn ferrite and of ZnO in a stainless-steel autoclave reactor (4848 Parr reactor), with mechanical stirring, useful volume of 100 mL, and working with maximum pressure of 200 bar, under the same synthesis conditions adopted to the magnetic stirring reactor.

2.3. Characterization

All catalysts obtained were characterized by: - X-ray diffraction (XRD) using a BRUKER X-ray diffractometer (D2 PHASER model, Cu-Kα radiation), operating with copper target tube at voltage of 30.0 kV and 10.0 mA current, with 55D160 detector; - Thermogravimetric analysis (TG/DTG) using Perkin Elmer STA 6000 TG-DTA equipment in N_2 atmosphere with flow of 20 $mL.min^{-1}$ and heating rate of 10 $°C.min^{-1}$, using 10 mg of sample in alumina crucible, and temperature range from 30 to 850 °C; - Density by helium (He) gas pycnometry, performed on a Upyc 1200e v5.04 Pycnometer, manufactured by Quantachrome Corporation; - Scanning electron microscopy using field emission (SEM/FEG) on a Philips brand microscope, model XL30 FEG; - Analysis of magnetic measurements, using a Lake Shore Model 7404 Vibrating Sample Magnetometer (VSM) with a maximum applied magnetic field of 13,700 G at room temperature; - Particle size distribution using the laser diffraction technique on SZ-100 series nanoparticle analyzer (HORIBA Scientific); - Textural analysis by nitrogen adsorption (BET), using the surface area and pore size analyzer, Quantachrome brand, Nova 3200 model.

Soybean oil and products resulting from catalytic tests were characterized regarding acidity according to the official AOCS method (Cd 3d-63). All products from the catalytic tests were analyzed regarding percent conversion to ethyl esters using a VARIAN 450c gas chromatograph, with flame ionization detector, and Varian Ultimetal (Select Biodiesel Glycerides + RG) stationary phase capillary column (15 m × 0.3 2 mm × 0.45 m).

3. Results and discussion

3.1. Characterization of the catalysts

Fig. 1 shows the diffractograms of the Ni-Zn ferrite synthesized by combustion in the pilot plant, (a) with standard heating reactor (FNZ) and (b) with a second heating reactor higher power 4000 W (FNZR2).

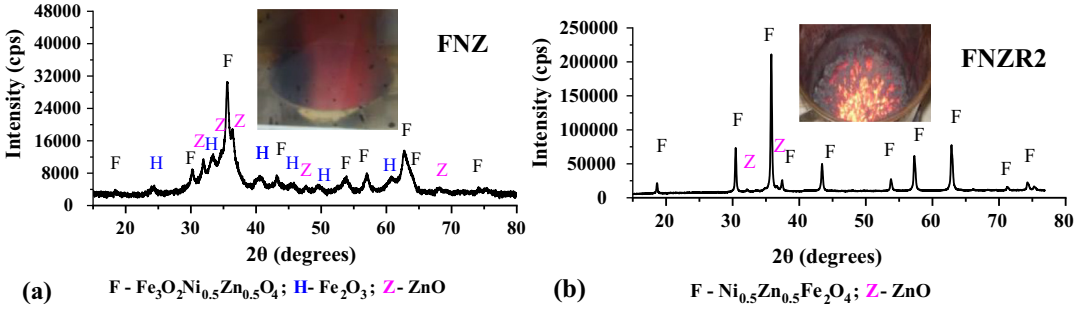

Fig. 1 Diffractograms of the Ni-Zn ferrite synthesis product in (a) pilot plant standard heating reactor (FNZ) and (b) higher power heating reactor (FNZR2).

Based on Fig. 1a, it is possible to observe that a low crystallinity polyphase system was formed characterized by the presence of the phase of interest, the cubic crystal structure of the inverse spinel $Ni_{0.5}Zn_{0.5}Fe_2O_4$ identified by the standard data card PDF 01–072-6799, besides the presence of secondary phases: iron oxide (Fe_2O_3) in the rhombohedral crystalline phase of hematite (standard card PDF 01–087-1165), and hexagonal zinc oxide (ZnO) (standard card PDF 01–089-1397). In a study by Dantas et al. (2018), where seeking to obtain the system $Ni_{0.5}Zn_{0.5}Fe_2O_4$, the same behavior of hematite and ZnO secondary phases presence was observed, but reached an average combustion temperature of 800 °C, therefore, it is believed that the formation of secondary phase in the final product it may be related to the large quantities of gases formed during combustion explosions as a result of the low combustion temperature reached (388 °C).

In order to reach higher combustion temperatures, the ferrite Ni-Zn (FNZR2) was synthesized using a second reactor with higher heating power (4000 W), which led to a higher combustion temperature of 659.7 °C and a burning in the coal form. This may have caused a slower burning during the reaction, and thus promoted gas elimination, reducing the effect of the explosion on flame combustion. Thus, as illustrated in the diffractogram (Fig. 1b), there was the formation of the system $Ni_{0.5}Zn_{0.5}Fe_2O_4$, with higher crystallinity and less amount of secondary phase, with only traces of the phase ZnO. Thus, the increase of the reactor heating power was efficient, since it directly affected the combustion temperature, and even the obtained product presenting reaction and crystalline characteristics different from the initial reproducibility parameter (Dantas et al., 2018), allowing to obtain a diphasic system from the combustion reaction.

Thermogravimetric events (TG/DTG) were performed only for ferrite Ni-Zn (FNZ) synthesized in the pilot plant with standard heating reactor in order to observe the thermal stability temperature and the obtained curves are illustrated in Fig. 2 from which we may determine decomposition temperatures and mass losses (%).

From the TG/DTG curves obtained for the ferrite Ni-Zn sample (FNZ) it was possible to observe three basic stages of mass loss. The first stage occurred in the range from 27 to 299 °C with mass loss of 3.1% associated with water and adsorbed gases. The second stage occurs between 299 and 445 °C with a loss of 1.1%. It can be attributed to the decomposition of completely non decomposed nitrate residues in combustion, since they are known to have explosive properties

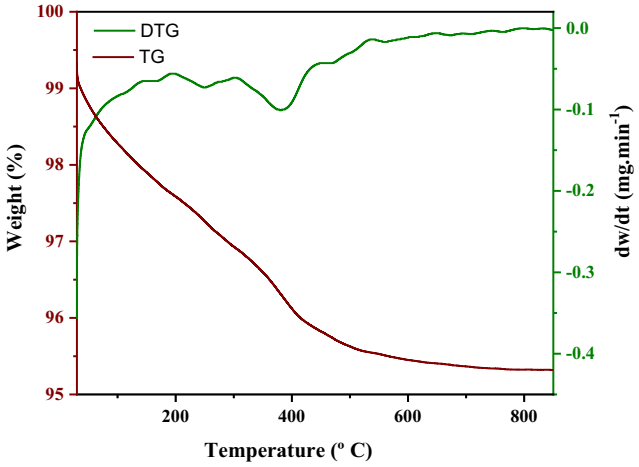

Fig. 2 TG/DTG curves of Ni-Zn ferrite synthesis product obtained in the standard heating reactor from the pilot plant (FNZ).

and they are very evident at elevated temperatures (Olhero et al., 2012; Ramesh et al., 2016). The third stage occurs between 445 and 800 °C when it reaches thermal stability, with little change in mass loss 0.5%, which may correspond to the recrystallization of the spinel phase under study.

Considering that the combustion temperature of the FNZR2 catalyst synthesis was 659.7 °C and the thermal stabilization temperature of the FNZ polyphase catalyst according to the thermogravimetric analysis of around 800 °C, it was subjected to a heat treatment at a temperature of 800 °C, using the rapid heating rate of 20 °C/min with only 5 min of burning time, thus completely eliminating the secondary phases and thus forming the single-phase composition of the system $Ni_{0.5}Zn_{0.5}Fe_2O_4$.

The X-ray diffractograms obtained are shown in Fig. 3: (a) FNZ ferrite calcined at 800 °C (FNZ_C) and (b) Zinc oxide synthesized by combustion reaction in the higher power heating reactor.

The diffractogram of the FNZ_C sample (Fig. 3a) indicates that the inverse spinel single-phase system $Ni_{0.5}Zn_{0.5}Fe_2O_4$ was achieved after calcination of the polyphase FNZ ferrite sample, indicating that the temperature of 800 °C was efficient for eliminating the secondary phases of hematite and ZnO. These results, combined with the reports and experiences of work already developed by our research group in recent years,

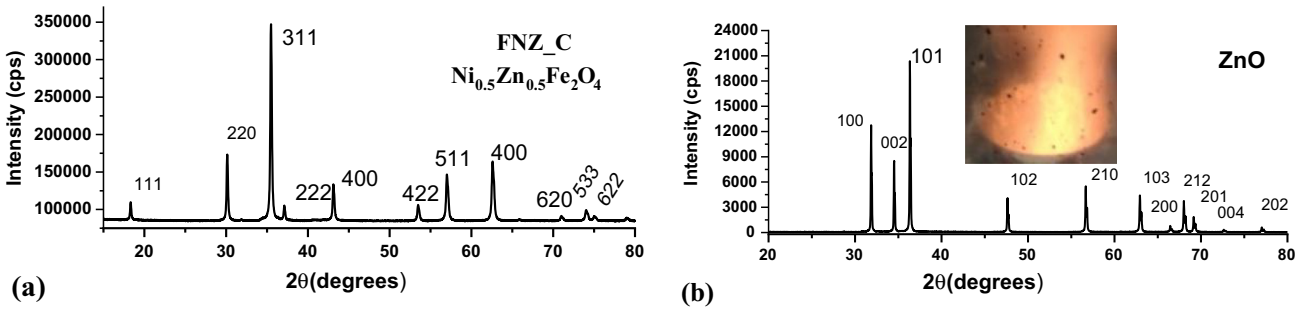

Fig. 3 X-ray diffractogram of the catalysts: (a) FNZ_C - $Ni_{0.5}Zn_{0.5}Fe_2O_4$ system and (b) ZnO.

which has been producing different types of ferrites on a large scale by combustion reaction (Mapossa et al., 2020; Torquato et al., 2018; Leal et al., 2018; Dantas, et al., 2018; Dantas, J. et al., 2017), prove the need and importance of reaching high reaction temperatures (> 800 °C) to obtain single-phase ferrites directly from the combustion reaction (Dantas, et al., 2017; Diniz et al., 2014). And in cases where combustion occurs at moderate temperatures (< 600 °C), the calcination after reaction can promote the formation of the desired single-phase ferrite (Diniz et al., 2014; Santos, et al., 2014; Chauhan et al., 2016).

It was also observed by the diffractogram (Fig. 3b), the obtaining of pure ZnO that was synthesized after changing the pilot plant reactor and it also occurred without the release of large amounts of gases, reaching a maximum temperature of 897 °C, similar behavior to that observed for ferrite FNZR2, thus indicating that the control of temperature and consequently the reaction time may be the determining factor during the synthesis by combustion reaction, in particular with regard to the direct obtaining of the single-phase $Ni_{0.5}Zn_{0.5}Fe_2O_4$ system.

In the study by Söllradl et al. (2015), the synthesis and characterization of colored ZnO-based powders is reported via solution combustion method (SCM), which also used urea as the reaction fuel and zinc nitrate hexahydrate as a metallic precursor, however, carried out a study of the effect of the molar ratios of these reagents (varying between 1:1 and 10:1) to obtain N-doped ZnO. However, they reported that the doping of significant amounts of nitrogen and hydrogen was only possible in the sample with molar ratio of 2.3:1, while that in lower proportions (1:1), they showed how difficult was a reliable interpretation of the localization of the investigated elements, since using the combination of the surface (XPS - X-ray photoelectron spectroscopy) and bulk sensitive (PGAA - Prompt Gamma Activation Analysis) techniques showed that the quantification and identification of Nitrogen was below or close to the detection limits of the equipment.

The ZnO obtained in the present study has similar characteristics to that obtained in the study by Söllradl et al. (2015), with molar ratio of 1:1 of urea and zinc nitrate hexahydrate, since both presented the hexagonal ZnO formation with wurtzite crystalline structure and salmon-pink color. An indicative that the amount of fuel used (calculated using the method described by Jain et al., 1981) was adequate (in the present study with stoichiometric coefficient, $\varphi = 1$, and molar ratio fuel/metallic precursor equivalent to ± 1.67:1), once it was not used fuel in deficiency and neither in excess, it was the non-formation of secondary phases arising from organic decomposition products of the precursor reagents.

Table 1 shows the structural characteristics of the catalysts obtained by X-ray diffraction data and He_2 pycnometry, such as crystallite size, crystallinity and density. The data made it possible to verify that the highest crystallinity and crystallite size were obtained for the samples FNZ_C and ZnO, which is related to the higher temperatures to which they were submitted, attesting that the increase in temperature directly influences these characteristics.

A possible influence of the secondary phases on the relative density characteristics was also noticed, since the FNZ sample was the catalyst that presented the lowest density and it has hematite in its crystalline composition, and as the Fe_2O_3 phase has lower density than the one Ni-Zn ferrite phase, this explains the lower relative density of this sample. FNZR2 ferrite presented higher relative density among the studied catalysts, which may be related to the presence of ZnO still as a secondary phase in its composition and which in turn has higher density than hematite and pure Ni-Zn ferrite.

The efficiency of the combustion reaction method for the synthesis of these materials is also proven by Dantas et al. (2020) and Mapossa et al. (2020) who obtained the respective systems: $Ni_{0.5}Zn_{0.5}Fe_2O_4$ in polyphasic form (with the presence of ZnO and Fe_2O_3 phases) and $Ni_{0.3}Zn_{0.7}Fe_2O_4$, these with average crystallite sizes of 37 and 20 nm and average crystallinity of 62.5 and 72.0%, respectively, presenting similar characteristics to that observed for the samples FNZ and FNZR2 in the present study.

The structural and surface characteristics (specific surface area - S_{BET}, particle size - D_{BET}, pore volume - V_P and pore diameter - D_P) for the samples FNZ, FNZR2, FNZ_C and ZnO are shown in Table 2.

The surface parameters (Table 2) of the FNZ sample compared to the FNZR2 and FNZ _C samples indicate that both pilot plant reactor modification and heat treatment promoted a reduction in surface area and pore volume. The obtaining of ZnO by combustion promoted the formation of a smaller surface area and smaller pore volume among the synthesized catalysts. This reduction in surface measures may be due to the elimination of secondary phases and possible carbon segregated traces of the surface of Ni-Zn ferrite from incomplete burning of reagents used during synthesis. However, these data are in agreement with the increase in the degree of crystallinity and crystallite size observed in Table 1.

A similar behavior was observed by Lv et al. (2016) when they synthesized one-dimensional isolated $Ni_{0.5}Zn_{0.5}Fe_2O_4$

Table 1 Crystallite size (D) and crystallinity of the Ni-Zn (FNZ, FNZR2 and FNZ_C) and zinc oxide samples, and their respective experimental densities, ρ_{Exp} (g/cm^3), obtained from He_2 pycnometry analysis, and the relative density DR (%).

Sample	2θ (°)	D (nm)	Crystallinity (%)	ρ_{Exp} (g/cm^3)	*D_R (%)
FNZ $_{(3\ 1\ 1)}$	35.5	22.8	62.9	5.12	95
FNZR2 $_{(3\ 1\ 1)}$	35.7	40.2	74.4	5.55	103
FNZ_C $_{(3\ 1\ 1)}$	35.4	43.0	92.2	5.37	100
ZnO $_{(1\ 0\ 1)}$	36.5	63.6	90.3	5.54	98

* $D_R = (\rho_{Exp} / \rho_{Theoretical})$ x100%, where $\rho_{Theoretical}$ is the theoretical density, ρ (g/cm^3), from the crystallographic records: ZnO (5.67 g/cm^3), $Ni_{0.5}Zn_{0.5}Fe_2O_4$ (5.36 g/cm^3) and Fe_2O_3 (5.28 g/cm^3).

Table 2 Results of textural analysis obtained from N_2 adsorption measurements for FNZ, FNZR2, FNZ_C and ZnO samples.

Sample	S_{BET} (m^2/g)	V_P (cm^3/g)	D_P (nm)	*D_{BET} (nm)	**D_{BET} (nm)	*D_{BET}/D_{XRD}
FNZ	56.8	0.048	3.3	20.6	19.6	0.9
FNZR2	14.2	0.015	3.4	76.1	78.5	1.9
FNZ _C	7.0	0.007	3.4	159.6	159.3	3.7
ZnO	5.2	0.005	3.4	208.3	203.5	3.3

* Values obtained using the experimental densities ρ (g/cm^3) from He gas pycnometry analysis;
** Values obtained using the theoretical densities ρ (g/cm^3) from the standard crystallographic data.

microtubes via a template assisted sol–gel method and evaluated the influence of calcination temperature on the structural and magnetic properties of the obtained NiZn ferrites microtubes. The authors observed that the increase in calcination temperature from 600 to 1000 °C caused a decrease in the specific surface area from 80.7 to 17.0 m^2/g due to an increase of the grain size from 25.3 to 112 nm.

However, the same pore diameter was observed for all obtained catalysts, with values around 3 nm, which is within the range of 2 to 50 nm, in accordance with the values established by IUPAC for pore diameter in solid structures, indicating that they have disordered surface characteristics with nonporous regions and other regions that have mesoporous with various types of shapes and sizes (Alothman, 2012).

The lowest mean particle diameter/mean crystallite diameter (D_{BET}/D_{XRD}) ratio was 0.9 for the FNZ sample, close to 1.0, suggesting the formation of a monocrystalline material. However, ferrites are characterized as polycrystalline materials (Arboleda et al., 2018), which is evidenced and confirmed by the results of the diphasic (FNZR2) and single-phase (FNZ_C) samples that have *D_{BET}/D_{XRD} values of 1.9 and 3.7, respectively, suggesting the interference of the secondary phases in these data. For the single-phase ZnO sample, the *D_{BET}/D_{XRD} ratio was 3.3 and therefore greater than 1.0, also characterizing polycrystalline material.

Estimates of mean particle size and particle size distribution were obtained by the dynamic light scattering technique and the cumulative (blue) curves of the cluster distribution range and the frequency (black) histograms of the distribution of same diameter clusters obtained for the FNZ, FNZR2, FNZ_C and ZnO samples are shown in Fig. 4. In addition, we can see the median particle diameters (point separating the cumulative frequency curve into two equal halves, D (50%), the diameters related to the cutting of the cumulative distribution curve D(10%) and the D(90%) and the scanning electron microscopy (SEM) images.

From the histograms (Fig. 4) it was possible to observe that all the samples presented frequency of asymmetric trend particle size, with values smaller than the mode (center point), and single modal behavior (characteristic of homogeneous particle sizes), except for the FNZ sample that showed.

These data associated with the SEM images in Fig. 4 are in common agreement and show the influence of the presence of secondary phase on crystalline, morphological and superficial characteristics, being in agreement with the observed XRD data, indicating that the temperature reached with the change made in the power of heating of the reactor and the heat treatment provided contributed to the elimination of secondary hematite and ZnO phases possibly formed on the surface or segregated into the main phase of the FNZ catalyst (Fig. 4a).

However, as the sample temperature increases, the characteristics of fine flocculated particles, similar to fragile blocks with high porosity, that is, become thicker, smaller in porosity, and large uniformity in particle agglomerate sizes (Fig. 4b and c), thus evidencing the elimination of the residue of organic matter present in the Ni-Zn ferrite derived from direct synthesis.

As for the zinc oxide micrograph obtained separately by combustion reaction, there is a growth of stems in multiple directions along a flat surface of the faces leading to the formation of a morphology similar to a cluster of flowers formed by smooth and small plates.

Similar characteristics to that observed in the study by Söllradl et al. (2015), in which they report the morphology of ZnO sample powders synthesized by combustion reaction with a hexagonal ZnO pyramid particles.

The observed mean, mode and median values are approximate for all samples, FNZ, FNZR2, FNZ_C and ZnO, are

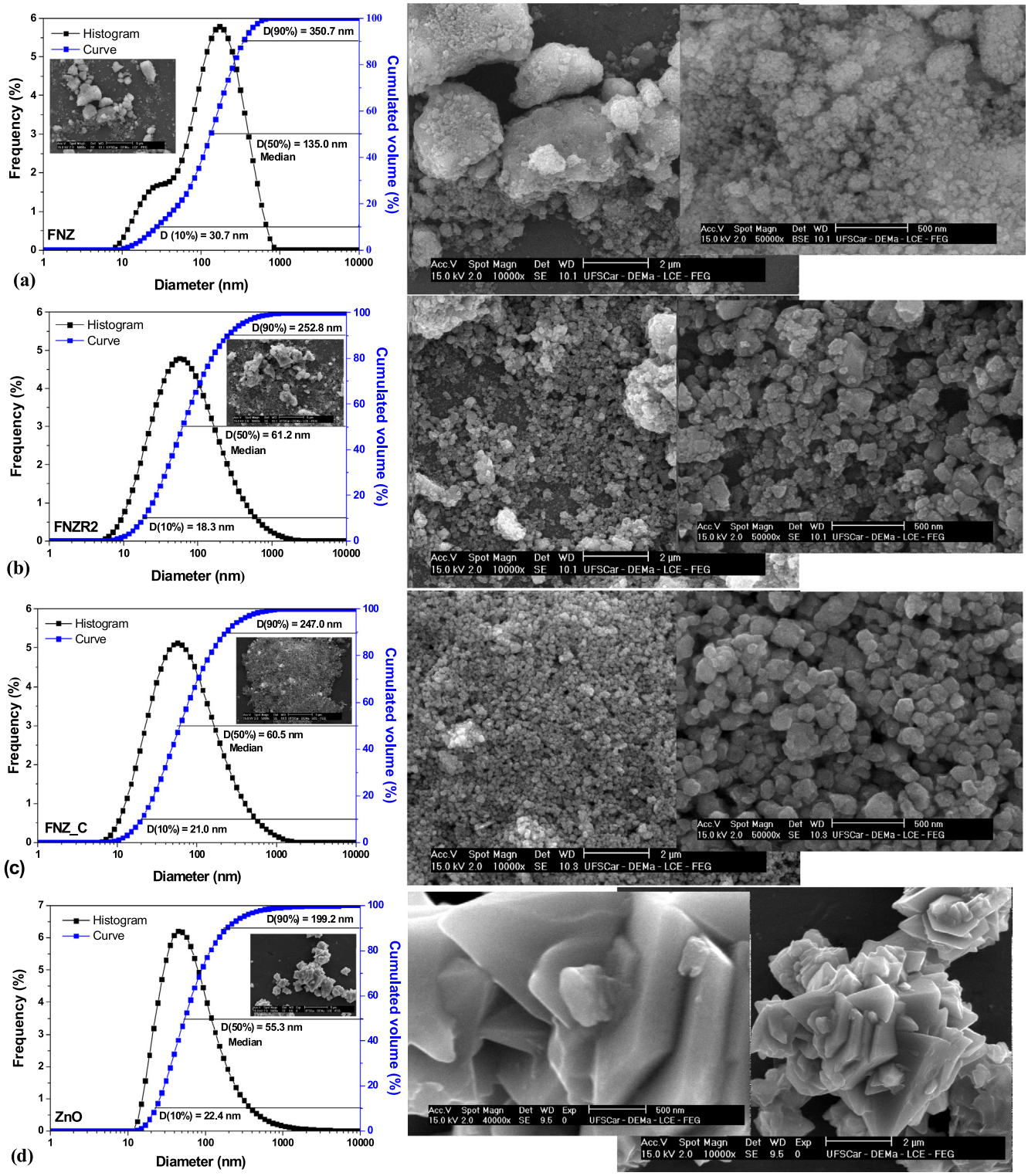

Fig. 4 Particle size distribution and scanning electron microscopy of the catalysts: a) FNZ, b) FNZR2, c) FNZ_C and d) ZnO.

within the cumulative volume range of particle size distribution D90% and D10% (Table 3), indicating that of in general, combustion synthesis results in a material with granulometric characteristics, with statistical variations that corroborate the other performed characterizations. The samples FNZR2, FNZ_C and ZnO also presented values of median particle size, D(50%), smaller than 100 nm, which makes it possible to classify as nanometric catalysts. However, different from the others, the FNZ sample was the only one to present characteristic of micrometric granulometry.

A large particle size distribution range was observed for all samples, with emphasis on FNZ and FNZR2 diphasic ferrite

Table 3 Values of mean, mode and median, besides the particle size distribution range referring to FNZ, FNZR2, FNZ_C and ZnO samples.

Sample	Mean (nm)	Mode (nm)	Median D50% (nm)	Particle size distribution accumulation range - D10%-D90% (nm)
FNZ	164.2	161.1	135.0	30.7–350.7
FNZR2	91.6	53.7	61.2	18.3–252.8
FNZ_C	71.4	53.7	60.5	21.0–247.0
ZnO	55.9	42.1	55.3	22.4–199.2

which showed higher distribution accumulation range, which is justifiable due to the presence of secondary phases, which due to the high energy surface of the ceramic powders, when in liquid medium, the Van der Waals forces act towards the destabilization of the suspensions, by the agglomerates formation (Dantas et al., 2017).

The magnetic properties were also evaluated for the FNZ, FNZR2 and FNZ_C catalysts, in order to observe which catalyst would contribute to the best magnetization in the reaction medium recovery process for possible reuse in catalysis. The magnetic hysteresis curves M × H, that is, the magnetization dependence M (emu/g) as a function of the applied magnetic field H (G) together with the saturation magnetization values (Ms), remnant magnetization (Mr) and coercive field (Hc) calculated from the catalyst hysteresis curves are shown in Fig. 5.

The hysteresis curves of the FNZR2 and FNZ_C catalysts illustrate the formation of very narrow, well-defined S-shaped magnetic hysteresis with low coercive field (Hc) and remnant magnetization (Mr) values indicating ferrimagnetic behavior characteristic of soft magnetic materials (magnetizes and degausses easily). The FNZ poly phase catalyst, although it had a low residual magnetization value (Mr), it was not observed the magnetization saturation point, suggesting a significant interference of the presence of secondary phase or even the crystallinity degree of the ferrites obtained in the catalyst magnetization process.

The highest saturation magnetization value was presented by the single-phase catalyst FNZ_C, however, the FNZR2 catalyst even with ZnO residue still had a good saturation magnetization, with only 8.6 emu/g less than the FNZ_C ferrite, which suggests for both catalysts, a good magnetic

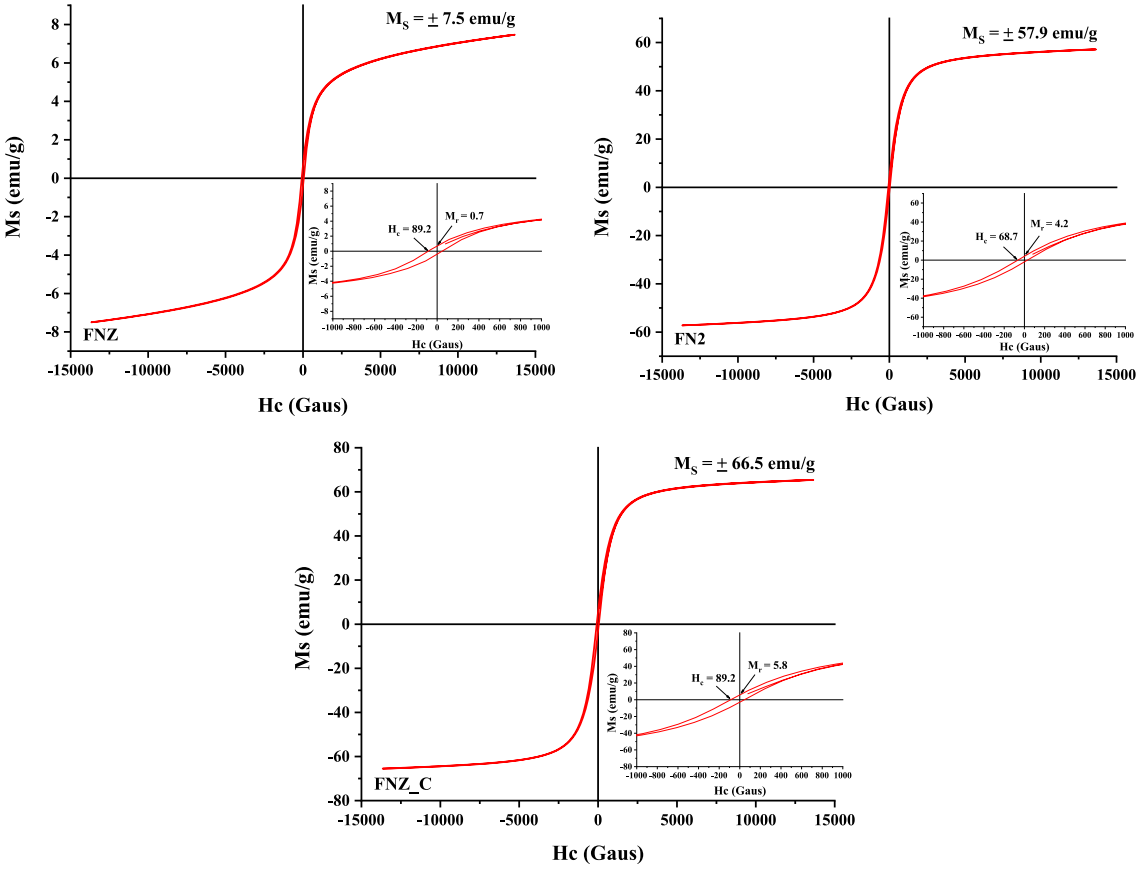

Fig. 5 Hysteresis parameters based on the M × H hysteresis magnetic curve and their respective magnifications to determine the Mr (remnant magnetization) and Hc (coercive field) of the FNZ, FNZR2 and FNZ_C samples.

contribution in the separation and/or recovery process of the catalyst from the reaction medium for possible reuse in catalysis. As observed in the present study and also reported by Lv et al. (2016), there is a significant influence of the obtaining and calcining temperature on the structural and magnetic properties of $Ni_{0.5}Zn_{0.5}Fe_2O_4$-based materials, since the samples demonstrate greater magnetization after subjected to high calcination temperatures.

3.2. Characterization of the catalytic test products

3.2.1. Catalytic evaluation of the catalysts in magnetic stirring reactor

In order to evaluate the effect of the reaction stirring mechanism, the catalytic tests were initially performed using magnetic stirring on biodiesel production, and thus to evaluate the interference of the magnetic property of the poly phase catalyst FNZ and single-phase catalyst FNZ_C on the conversion of soybean oil to ethyl esters. The ester conversion results obtained from the catalytic test products are shown in Fig. 6.

As shown in Fig. 6a, the FNZ catalyst promoted a significant ester conversion 78.2 ± 0.3%, while the FNZ_C catalyst promoted a lower catalytic activity, with only 23.9 ± 2.5% ester conversion which represents a reduction of 54.3% in catalyst activity when using the FNZ_C catalyst. This reduction indicates a greater interference of the catalyst magnetization of FNZ_C with catalyst FNZ, as observed in Fig. 5. After catalytic reactions these magnetic characteristics are also evident, since part of the catalyst FNZ clings to the magnetic stirring bar, while the entire catalyst FNZ_C clings to the magnetic bar, as illustrated in Fig. 6a, thus indicating that the catalyst is unable to participate fully in the reaction because of magnetization interference. This effect has also been reported in the literature as a possible interfering effect on conversion, since the studied ferrites had magnetic characteristics in the range between 19 emu/g (Dantas et al., 2020) and 55 emu/g (Dantas et al., 2017).

From the acidity index analysis performed for the oil and obtained biodiesels (Fig. 6b), it is clear that the starting oil for biodiesel production has an acidity of 1.7 mg of KOH/g of sample, the value still within the recommended limits for use in biodiesel production, because in this process by homogeneous alkaline catalysis, the oil used must have specific properties in which the free fatty acid content should not exceed 1% by mass (Carrero et al., 2015; Aboelazayem et al., 2019). After the catalytic tests it was observed that the biodiesel produced using the catalysts FNZ and FNZ_C maintained basically the same acidity of the oil, with only a deviation of ± 0.4 mg KOH/g, indicating that the free fatty acids present in the starting oil were not consumed and, therefore, there was no complete conversion of fatty compounds, remaining them free in the final product.

3.2.2. Catalytic evaluation of the catalysts in mechanical stirring reactor

In order to better study the catalytic behavior of the obtained catalysts, we tried to eliminate the magnetic interference and proposed to evaluate the interference of the secondary phase on the catalytic activity of Ni-Zn ferrite. For this the catalytic tests were performed using the mechanical stirring reactor (Parr type reactor) and the catalysts: polyphasic (FNZ), diphasic (FNZR2) and monophasic (FNZ_C), besides the mass ZnO as this is the secondary phase that makes up the catalyst FNZR2. The reaction conditions used in the magnetic stirring reactor tests were maintained. The results of these catalytic tests are illustrated in Fig. 7.

Although there is a proven catalytic activity of ZnO in biodiesel production when tested in mass way (Lamba et al., 2019; Laskar et al., 2019; Dutta et al., 2019), as well as a proven catalytic activity of the $Ni_{0.5}Zn_{0.5}Fe_2O_4$ polyphasic system (with presence of ZnO and Fe_2O_3) obtained direct from the combustion reaction (Dantas et al., 2018; Dantas et al., 2020), in agreement with the results obtained in the present study (Fig. 7a), which reinforces the questioning never before evaluated, which is the phase ($Ni_{0.5}Zn_{0.5}Fe_2O_4$, ZnO or Fe_2O_3) that would really have greater influence on the conversion into esters when the polyphasic system is applied as catalyst in the production of biodiesel.

Thus, from the tests carried out in the Parr reactor (Fig. 7a), it was possible to observe that the catalysts FNZ (polyphasic: $Ni_{0.5}Zn_{0.5}Fe_2O_4$, ZnO and Fe_2O_3), FNZR2 (diphasic: $Ni_{0.5}Zn_{0.5}Fe_2O_4$ and ZnO), and FNZ_C (single-phase: $Ni_{0.5}Zn_{0.5}Fe_2O_4$) promoted excellent conversions in esters with close values, with no significant variation in

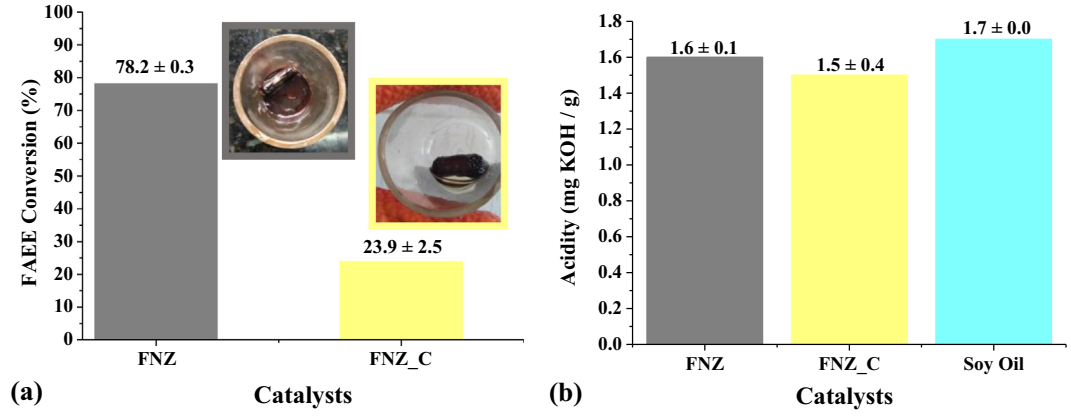

Fig. 6 Conversions obtained from catalytic tests performed using magnetic stirring with the catalysts FNZ and FNZ_C (a); and the acidity values of the oil and the obtained biodiesels (b).

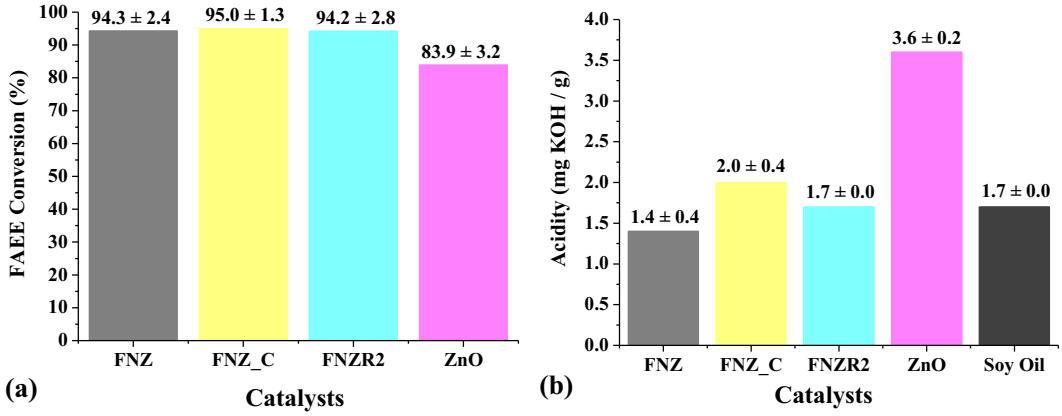

Fig. 7 Catalytic conversion for transesterification reactions using the catalysts FNZ, FNZ_C, FNZR2 and ZnO, tested on the mechanical stirring reactor (a), and the values of acid index of the oil and the obtained biodiesels (b).

catalytic activity for the different catalysts evaluated. And, although ZnO also promoted a good conversion to esters (83.9 ± 2.8%), the similarity of the results in the catalytic effectiveness obtained from the evaluated Ni-Zn ferrites (with or without the presence of a secondary phase) made it possible answer the question highlighted in this study, since it indicates that the high conversion to esters is promoted by the $Ni_{0.5}Zn_{0.5}Fe_2O_4$ system, since its catalytic activity is independent of the existence of the oxides present as secondary phases, and therefore, presenting enough active sites for accelerate the transesterification reaction.

Another factor never before evaluating that it was sought to study in the present work, it was the influence of the magnetic property of the catalysts on the catalytic behavior, in which, from the results of the catalytic tests using the catalysts FNZ and FNZ_C carried out in the mechanical stirring reactors (Fig. 7a), compared to the tests performed under magnetic stirring (Fig. 6a), it was observed a significant difference in the catalytic activity, with an increase in the conversion values when the tests were performed in a reactor with mechanical stirring. This confirms that the magnetization force of the catalyst used can be a determining factor in the catalytic effect and, therefore, for catalysts with magnetic properties it is essential that the reaction be carried out without the interference of the magnetic stirring so that the catalyst can be free to participate of the reaction.

It is also important to highlight that the work by Dantas et al. (2017) and Dantas et al. (2020) reported in the literature, evaluated the catalytic activity in the biodiesel production of the $Ni_{0.5}Zn_{0.5}Fe_2O_4$ system with magnetic characteristics of 55 emu/g and 36 emu/g, which achieved conversions of 5.5 and 14% in methyl transesterification of soybean oil, respectively. Although the aforementioned studies have been evaluated under different reaction conditions than those adopted in the present study, it can be confirmed the interfering effect of the magnetic characteristic of NiZn ferrite on the catalytic conversion of the reaction, since these were carried out under the action of a magnetic stirring, preventing the effective participation of these ferrites in the evaluated reactions.

Rosen (2018) highlighted the need for a careful and serious consideration of the environmental sustainability aspects of this sector of the biofuels industry, as although these address the concern with energy and environmental issues in their activities, waste is also generated that potentially affects the environment and human health. In this context, it reports the need of researches that use methods and indicators that aim to help in determine the most efficient ways of synthesis and consumption patterns in terms of resources, with cost effective and ecologically benign to the environment. Among the various methods mentioned by Rosen (2018), the one based on life cycle assessment (LCA) when applied to biodiesel production has been widely reported by researchers looking to replace homogeneous catalysis (Wang et al., 2017; Guldhe et al., 2017; Booramurthy et al., 2019; Teo et al., 2019) by catalytic processes that promote the recovery and reuse of solid catalysts.

The evaluation of the reuse cycles of ferrite-based catalysts after proven efficiency in biodiesel production was well reported by Dantas et al. (2020), Alaei et al. (2018), Falcão et al. (2018), and Ashok and Kennedy (2019); however, in the present study it was not evaluated, since among the studies cited, the one by Dantas et al. (2020) stands out for proving that the use of Ni-Zn ferrite is promising in the biodiesel production when evaluating the reuse of the $Ni_{0.5}Zn_{0.5}Fe_2O_4$ system, thus confirming the average conversion capacity of 98,9% even after three cycles of reuse in the SET reaction (simultaneous esterification and transesterification) by methyl route.

In view of these results, it is also important to highlight that although a high surface area is fundamental in the catalysis, as widely highlighted in the literature (Madhawan et al., 2018), in the present study, this was not the determining factor in the conversion, since the surface area of FNZR2 and FNZ_C catalysts were lower than FNZ (reduction of 25.0 and 87.7% respectively), and they showed similar catalytic activity when tested in a mechanical stirring reactor. These data also indicate that active sites present in the evaluated catalysts are sufficient to promote good catalytic performance and must be freely available to participate in the reaction.

It was observed by Lamba et al. (2019), when they evaluated the catalytic behavior of ZnO obtained by different methods and conditions of synthesis, that the catalysts that had more basic active sites presented higher rates of reaction constants and, however, when the evaluated catalysts presented similar basic strength, the catalyst surface area promoted better performance. In addition, Lamba et al. (2019) also reported that a higher exposure of active oxygen ion in a specific ZnO morphology or any other properties of a catalyst, such as pore size, etc., can lead to improved rate constants for oxides with lower basic resistance and surface area.

The obtained results, therefore, allow to reaffirm that the magnetization of the catalysts associated with the stirring mechanism can influence the catalytic effectiveness, since it can reduce the availability of the different properties of the catalyst (surface area, pores and active sites) to participate of the reaction, therefore, it is necessary to use an appropriate stirring mechanism to promote a better mass transfer during the reaction, especially when the catalyst used has magnetic property.

The acidity indices (Fig. 7b) for the biodiesels produced with the FNZ, FNZR2, and FNZ_C catalysts in mechanical agitation maintained the same behavior observed in the magnetic agitation tests, with values close to or equal to the starting oil, indicating that part of the fatty acids was not consumed or even kept free in the final product. The catalyst ZnO had a much higher acidity than the starting oil indicating that there was a higher production of fatty acids in the reaction and they were not converted under the reaction conditions used.

The acidity index method was used to monitor the quality of biofuel obtained at the end of the reaction, since the maximum limit stipulated by the ANP for biodiesel is 0.5 mg KOH/g (ANP Resolution 42). And although the catalysts studied showed excellent conversions, there is still a need to optimize the reaction conditions to reach the optimal biodiesel quality limits established by the ANP.

4. Conclusions and future perspectives

The synthesis by combustion reaction using the pilot plant reactor was efficient in the reproducibility of the polyphasic $Ni_{0.5}Zn_{0.5}Fe_2O_4$ system (FNZ). The modification in the reactor heating power from the pilot plant, although it did not make it possible to obtain the single-phase ferrite in directly way, it still allowed to obtain the diphasic Ni-Zn ferrite (FNZR2), and it was also efficient in the large-scale ZnO synthesis. The heat treatment of the FNZ sample allowed to reach out a single-phase Ni-Zn ferrite (FNZ_C). The particle size and microscopy data indicated that the combustion reaction promotes the formation of a material with nanometric characteristics with low particle size asymmetry and the magnetic properties indicated a good magnetizing force to contribute to the process of separation and/or recovery of the catalyst from the reaction medium. The catalytic tests in the mechanical stirring reactor showed that Ni-Zn ferrite promoted optimum ester conversions of ± 94%, and although ZnO also promoted good ester conversion (83.9%), the results confirm that the catalytic effectiveness of Ni-Zn Ferrite is independent of secondary phases. The catalytic tests carried out in the magnetic stirring reactor made it possible to realize that the magnetic force can be a determining factor in the catalytic effectiveness of ferrites, since it can reduce the availability of the different properties of the catalyst (i.e., surface area, pores and active sites) to participate of the reaction, therefore, it is necessary to use an appropriate stirring mechanism to promote a better mass transfer during the reactions.

Thus, as future prospects for the consolidation of the $Ni_{0.5}Zn_{0.5}Fe_2O_4$ system as catalysts for biodiesel production, it is still necessary to better study the reaction conditions seeking to produce biodiesel in milder and more economic industrial conditions, that besides meet the conversion to esters, may also achieve good yield and the ideal limits of biodiesel quality established by the ANP, such as the acidity index.

Declaration of Competing Interest

The authors declare that they have no known competing financial interests or personal relationships that could have appeared to influence the work reported in this paper.

Acknowledgements

The authors thank CAPES/CNPq for their financial support.

References

Aboelazayem, O., Gadalla, M., Saha, B., 2019. Derivatisation-free characterisation and supercritical conversion of free fatty acids into biodiesel from high acid value waste cooking oil. Renew. Energy 143, 77–90.

Alaei, S., Haghighi, M., Toghiani, J., Vahid, B.R., 2018. Magnetic and reusable $MgO/MgFe_2O_4$ nanocatalyst for biodiesel production from sunflower oil: influence of fuel ratio in combustion synthesis on catalytic properties and performance. Ind. Crops Prod. 117, 322–332.

Ali, B., Yusup, S., Quitain, A.T., Alnarabiji, M.S., Kamil, R.N.M., Kida, T., 2018. Synthesis of novel graphene oxide/bentonite bi-functional heterogeneous catalyst for one-pot esterification and transesterification reactions. Energy Convers. Manage. 171, 1801–1812.

Alothman, Z.A., 2012. A review: fundamental aspects of silicate mesoporous materials. Materials 5 (12), 2874–2902.

AOCS. Official Method Cd 3d-63. Formerly Cd 3a-63. Reapproved, 2017.

Arboleda, J., Arnache, O., Aguirre, M., Ramos, R., Anadón, A., Ibarra, M., 2018. Evidence of the spin Seebeck effect in Ni-Zn ferrites polycrystalline slabs. Solid State Commun. 270, 140–146.

Ashok, A., Kennedy, L.J., 2019. Magnetically Separable Zinc Ferrite Nanocatalyst for an Effective Biodiesel Production from Waste Cooking Oil. Catal. Lett. 149, 3525–3542.

Ashok, A., Kennedy, L.J., Vijaya, J.J., 2019. Structural, optical and magnetic properties of $Zn1\text{-}xMnxFe_2O_4$ ($0 \leq x \leq 0.5$) spinel nano particles for transesterification of used cooking oil. J. Alloy. Compd. 780, 816–828.

Avhad, M., Marchetti, J., 2015. A review on recent advancement in catalytic materials for biodiesel production. Renew. Sustain. Energy Rev. 50, 696–718.

Baskar, G., Selvakumari, I.A.E., Aiswarya, R., 2018. Biodiesel production from castor oil using heterogeneous Ni doped ZnO nanocatalyst. Bioresour. Technol. 250, 793–798.

Booramurthy, V.K., Kasimani, R., Pandian, S., 2019. Biodiesel Production from Tannery Waste using a Nano Catalyst (Ferric-Manganese Doped Sulphated Zirconia). Energy Sources Part A, 1–13. https://doi.org/10.1080/15567036.2019.1639849.

Buchori, L., Istadi, I., Purwanto, P., 2017. Synthesis of biodiesel on a hybrid catalytic-plasma reactor over kˆsub2ˆo/CaO-ZnO catalyst. Sci. Study Res. Chem. Chem. Eng. Biotechnol. Food Industry 18, 303–318.

Carrera, Y., Morales-Mendoza, G., Valverde-Aguilar, G., Mantilla, A., 2013. $ZnO–Al_2O_3–La_2O_3$ layered double hydroxides as catalysts precursors for the esterification of oleic acid fatty grass at low temperature. Catal. Today 212, 164–168.

Carrero, A., Vicente, G., Rodríguez, R., del Peso, G.L., Santos, C., 2015. Synthesis of fatty acids methyl esters (FAMEs) from Nannochloropsisgaditana microalga using heterogeneous acid catalysts. Biochem. Eng. J. 97, 119–124.

Chagas, E., Ponce, A., Prado, R., Silva, G., Bettini, J., Baggio-Saitovitch, E., 2014. Thermal effect on magnetic parameters of high-coercivity cobalt ferrite. J. Appl. Phys. 116, 033901.

Chauhan, L., Shukla, A., Sreenivas, K., 2016. Properties of $NiFe_2O_4$ ceramics from powders obtained by auto-combustion synthesis with different fuels. Ceram. Int. 42, 12136–12147.

Costa, A., Kiminami, R., 2012. Dispositivo para a produção de manocompósitos cerâmicos em larga escala por reação de combustão e processo contínuo de produção de nanocompósitos. Revista Propriedade Industrial-RPI, BR 10 (2012). 002181-3.

Dantas, J., Leal, E., Cornejo, D., Kiminami, R., Costa, A., 2020. Biodiesel production evaluating the use and reuse of magnetic nanocatalysts $Ni_{0.5}Zn_{0.5}Fe_2O_4$ synthesized in pilot-scale. Arabian J. Chem. 13, 3026–3042.

Dantas, J., Leal, E., Mapossa, A.B., Silva, A.S., Costa, A.C.F.D.M., 2016. Síntese, caracterização e performance catalítica de nanoferritas mistas submetidas a reação de transesterificação e esterificação *via* rota metílica e etílica para biodiesel. Revista Matéria 21, 1080–1093.

Dantas, J., Leal, E., Mapossa, A., Cornejo, D., Costa, A., 2017. Magnetic nanocatalysts of $Ni_{0.5}Zn_{0.5}Fe_2O_4$ doped with Cu and performance evaluation in transesterification reaction for biodiesel production. Fuel 191, 463–471.

Dantas, J., Leal, E., Feitosa, A.C., Vasconcelos, E.V., Costa, A.C.F.D. M., 2018. Biodiesel from Fatty Acids Found in Brazilian Native Cultures as Soybean and Cotton Using the Nanocatalyst $Ni_{0.5}$-$Zn_{0.5}Fe_2O_4$. Mater. Sci. Forum. Trans. Tech. Publ., 274–279

Diniz, V.C.S., Vieira, D.A., Kiminami, R.H.G.A., Cornejo, D., de Melo Costa, A.C.F., 2014. Study of Temperature Sintering by Microwave Energy in Ferrites $Ni_{0.5}Zn_{0.5}Fe_2O_4$. Mater. Sci. Forum. Trans Tech. Publ., 410–414

Dutta, S., Jaiswal, K.K., Verma, R., Basavaraju, D.M., Ramaswamy, A.P., 2019. Green synthesis of zinc oxide catalyst under microwave irradiation using banana (Musa spp.) corm (rhizome) extract for biodiesel synthesis from fish waste lipid. Biocatal. Agricul. Biotechnol. 22, 101390.

Falcão, M.D.S., Garcia, M.A.S., Moura, C.V.R.D., Nicolodi, S., Moura, E.M.D., 2018. Synthesis, characterization and catalytic evaluation of magnetically recoverable $SrO/CoFe_2O_4$ nanocatalyst for biodiesel production from babassu oil transesterification. J. Brazil. Chem. Soc. São Paulo. 29, 845–855.

Farias, A.F.F., Moura, K.F., Souza, J.K., Lima, R.O., Nascimento, J.D., Cutrim, A.A., Longo, E., Araujo, A.S., Carvalho-Filho, J.R., Souza, A.G., 2015. Biodiesel obtained by ethylic transesterification using CuO, ZnO and CeO_2 supported on bentonite. Fuel 160, 357–365.

Guldhe, A., Singh, P., Ansari, F.A., Singh, B., Bux, F., 2017. Biodiesel synthesis from microalgal lipids using tungstated zirconia as a heterogeneous acid catalyst and its comparison with homogeneous acid and enzyme catalysts. Fuel 187, 180–188.

Jain, S., Adiga, K., Verneker, V.P., 1981. A new approach to thermochemical calculations of condensed fuel-oxidizer mixtures. Combust. Flame 40, 71–79.

Laskar, I.B., Rokhum, L., Gupta, R., Chatterjee, S. 2019. Zinc oxide supported silver nanoparticles as a heterogeneous catalyst for production of biodiesel from palm oil. Environ. Progr. Sustain. Energy, e13369.

Lamba, N., Gupta, R., Modak, J.M., Madras, G., 2019. ZnO catalyzed transesterification of Madhuca indica oil in supercritical methanol. Fuel 242, 323–333.

Lazarova, T., Kovacheva, D., Georgieva, M., Tzankov, D., Tyuliev, G., Spassova, I., Naydenov, A., 2019. Tunable nanosized spinel manganese ferrites synthesized by solution combustion method. Appl. Surf. Sci. 496, 143571.

Leal, E., Dantas, J., dos Santos, P.T.A., Bicalho, S.M.d.C.M., Kiminami, R.H.G.A., da Silva, M.R., de Melo Cost, A.C.F., 2018. Effect of the surface treatment on the structural, morphological, magnetic and biological properties of MFe_2O_4 iron spinels (M = Cu, Ni Co, Mn and Fe). Appl. Surf. Sci. 455, 635–645.

Lee, A.F., Bennett, J.A., Manayil, J.C., Wilson, K., 2014. Heterogeneous catalysis for sustainable biodiesel production *via* esterification and transesterification. Chem. Soc. Rev. 43 (22), 7887–7916.

Liu, F., Zhang, Y., 2011. Controllable growth of "multi-level tower" ZnO for biodiesel production. Ceram. Int. 37 (8), 3193–3202.

Lv, H.-N., Rebrov, E.V., Gao, P.-Z., Ma, R.-X., Lu, Z.-L., Xu, J., 2016. Controllable synthesis of one-dimensional isolated $Ni_{0.5}$-$Zn_{0.5}Fe_2O_4$ microtubes for application as catalyst support in RF heated reactors. Ceram. Int. 42, 7793–7802.

Madhawan, A., Arora, A., Das, J., Kuila, A., Sharma, V., 2018. Microreactor technology for biodiesel production: a review. Biomass Convers. Biorefin. 8, 485–496.

Mapossa, A.B., Dantas, J., Silva, M.R., Kiminami, R.H.G.A., Costa, A.C.F.M., Daramola, M.O., 2020. Catalytic performance of $NiFe_2O_4$ and $Ni_{0.3}Zn_{0.7}Fe_2O_4$ magnetic nanoparticles during-biodiesel production. Arabian J. Chem. 13, 3026–3042.

Olhero, S.M., Soma, D., Amaral, V.S., Button, T.W., Alves, F.J., Ferreira, J.M., 2012. Co-precipitation of a Ni–Zn ferrite precursor powder: Effects of heat treatment conditions and deagglomeration on the structure and magnetic properties. J. Eur. Ceram. Soc. 32, 2469–2476.

Pereira, K., Dantas, J., Dutra, R., Diniz, M., Silva, A., Costa, A.d.M., 2015. Synthesis of the Magnetic Nanoferrites of Spinel Type and Use in Esterification Reaction for Biodiesel Obtaining. Mater. Sci. Forum. Trans Tech. Publ., 125–130

Phadatare, M., Salunkhe, A., Khot, V., Sathish, C., Dhawale, D., Pawar, S., 2013. Thermodynamic, structural and magnetic studies of $NiFe_2O_4$ nanoparticles prepared by combustion method: Effect of fuel. J. Alloy. Compd. 546, 314–319.

Prasad, M.S.R., Babu, B.R., Ramesh, K., Trinath, K., 2014. Structural and magnetic studies on chromium substituted Ni-Zn nano ferrite synthesized by citrate Gel auto combustion method. J. Supercond. Novel Magn. 27, 2735–2745.

Ramesh, S., Dhanalakshmi, B., Sekhar, B.C., Rao, P.S., Rao, B.P., 2016. Structural and magnetic studies on Mn-doped Ni–Zn ferrite nanoparticles. Appl. Phys. A 122, 984.

Rosen, M.A., 2018. Environmental sustainability tools in the biofuel industry. Biofuel Res. J. 17, 751–752. https://doi.org/10.18331/BRJ2018.5.1.2.

Santos, P.T.A., Dantas, J., Araújo, P., Santos, P., Costa, A., 2014. The Influence of Calcination Temperature in Ni-Zn Ferrite Doped with Al^{3+}. Materials Sci. Forum. Trans Tech Publ., 399–403

Shan, R., Lu, L., Shi, Y., Yuan, H., Shi, J., 2018. Catalysts from renewable resources for biodiesel production. Energy Convers. Manage. 178, 277–289.

Söllradl, S., Greiwe, M., Bukas, V.J., Buchner, M.R., Widenmeyer, M., Kandemir, T., Zweifel, T., Senyshyn, A., Günther, S., Nilges, T., 2015. Nitrogen-doping in ZnO via combustion synthesis?. Chem. Mater. 27, 4188–4195.

Tang, Z.-E., Lim, S., Pang, Y.-L., Ong, H.-C., Lee, K.-T., 2018. Synthesis of biomass as heterogeneous catalyst for application in biodiesel production: State of the art and fundamental review. Renew. Sustain. Energy Rev. 92, 235–253.

Teo, S.H., Islam, A., Chan, E.S., Choong, S.T., Alharthi, N.H., Taufiq-Yap, Y.H., Awual, M.R., 2019. Efficient biodiesel production from Jatropha curcus using $CaSO_4/Fe_2O_3$-SiO_2 core-shell magnetic nanoparticles. J. Cleaner Prod. 208, 816–826.

Torquato, R., Shirsath, S., Kiminami, R., Costa, A., 2018. Synthesis and structural, magnetic characterization of nanocrystalline $Zn_{1-x}Co_xO$ diluted magnetic semiconductors (DMS) synthesized by combustion reaction. Ceram. Int. 44, 4126–4131.

Ullah, Z., Khan, A.S., Muhammad, N., Ullah, R., Alqahtani, A.S., Shah, S.N., Ghanem, O.B., Bustam, M.A., Man, Z., 2018. A review on ionic liquids as perspective catalysts in transesterification of different feedstock oil into biodiesel. J. Mol. Liq. 266, 673–686.

Wang, J., Wang, Z., Yang, L., Yang, G., Miao, C., Lv, P., 2017. Natural albite as a novel solid basic catalyst for the effective synthesis of biodiesel: Characteristics and performance. Energy 141, 1650–1660.